

Supporting Information

Table S1. Surface atomic ratio (C/N) determined by XPS spectra.

Samples	C/mol%	N/mol%	C/N
bulk g-C₃N₄	40.75	58.11	0.701
CMU	34.27	49.13	0.697
CMU-400	39.09	58.28	0.671
CMU-450	40.57	56.68	0.716
CMU-500	41.59	56.61	0.735
CMU-520	45.57	51.38	0.887

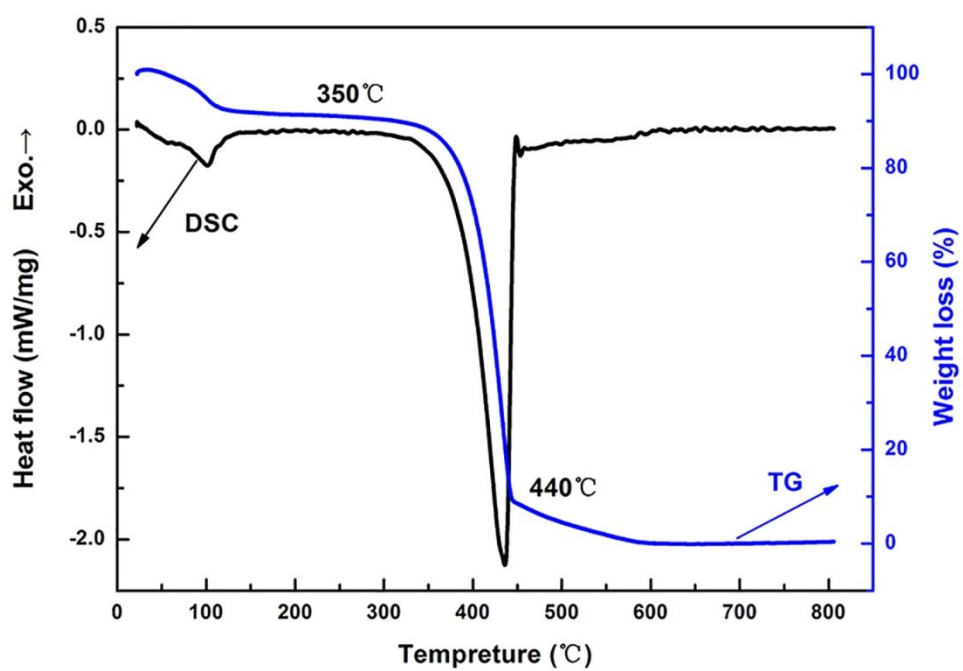


Figure S1. TG-DTA curve of CMU supramolecular self-assembly in the air atmosphere.

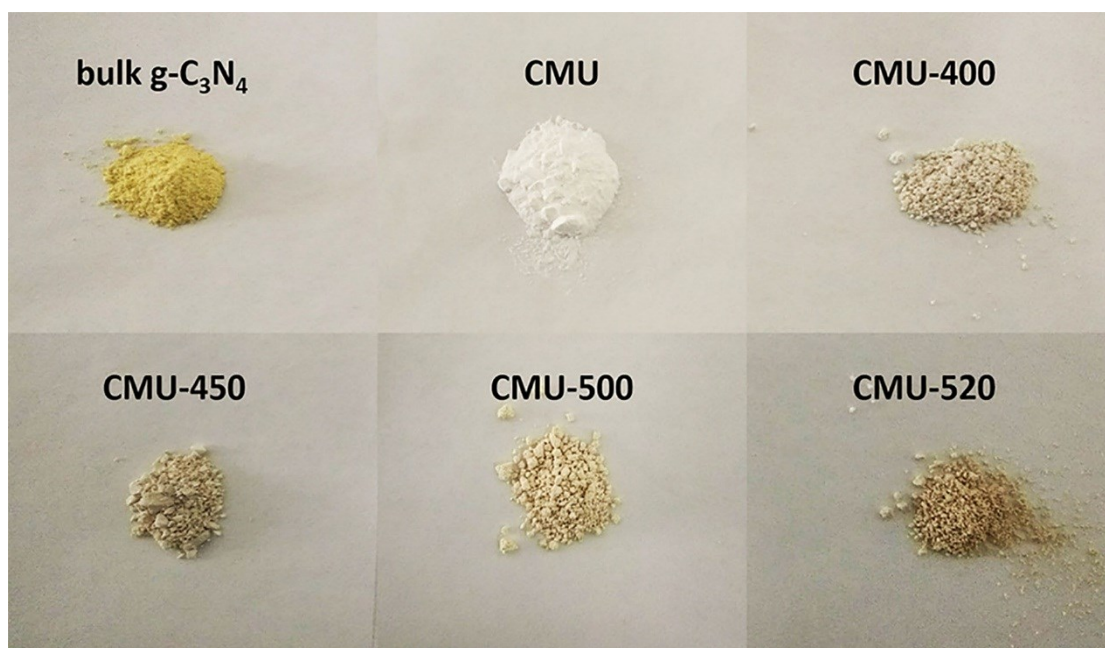


Figure S2. Photograph of obtained samples: bulk g-C₃N₄, CMU, and CMU-x.

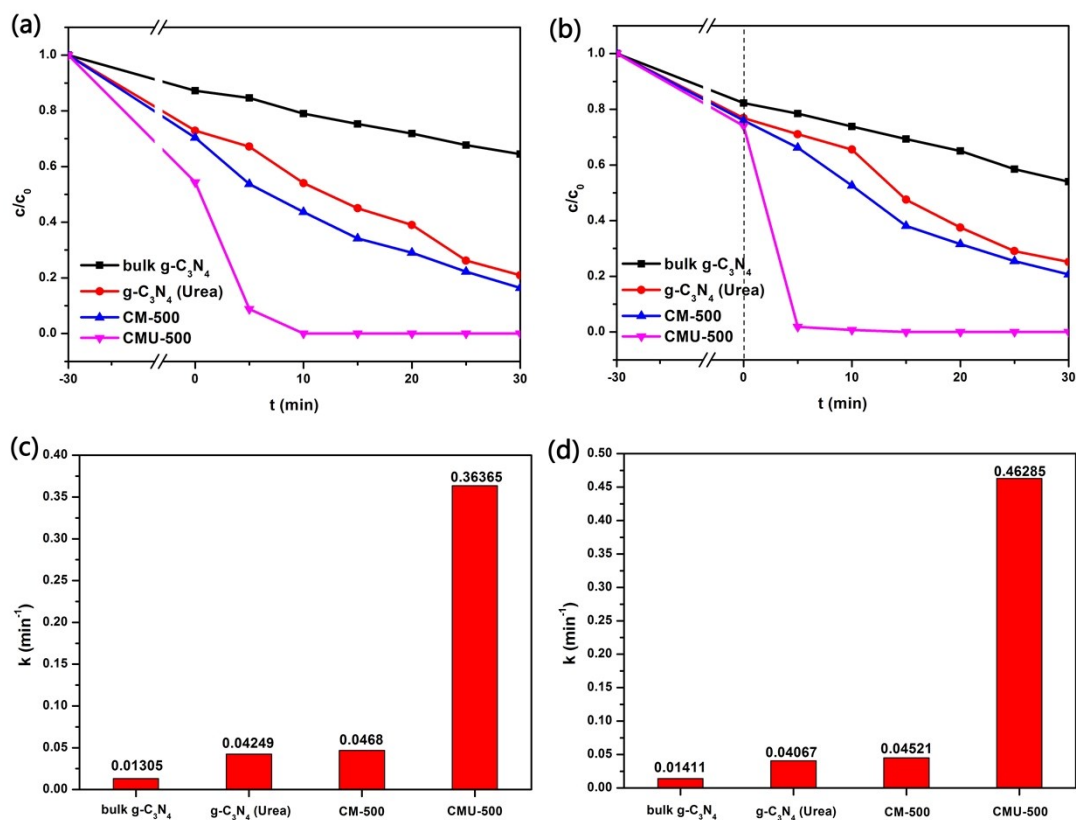


Figure S3. The residual fraction of (a) RhB and (b) Cr(VI) as a function of irradiation time with CMU-500 under visible light irradiation; (c) The concentration changes of RhB and Cr(VI) as a function of irradiation time with CMU-500 under visible light irradiation ($k > 420$ nm) without adding acid and (d) with adding H_2SO_4 (pH=1.82).

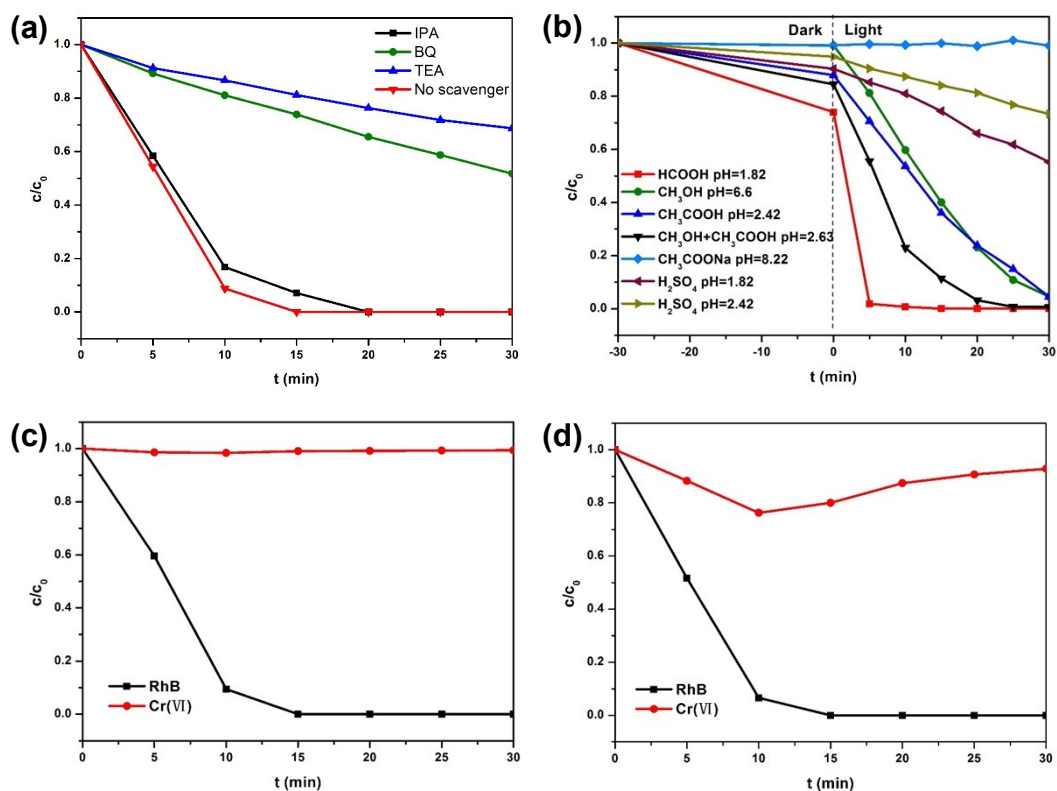


Figure S4. The residual fraction of (a) RhB and (b) Cr(VI) as a function of irradiation time with CMU-500 under visible light irradiation; (c) The concentration changes of RhB and Cr(VI) as a function of irradiation time with CMU-500 under visible light irradiation ($k > 420$ nm) without adding acid and (d) with adding H₂SO₄ (pH=1.82).

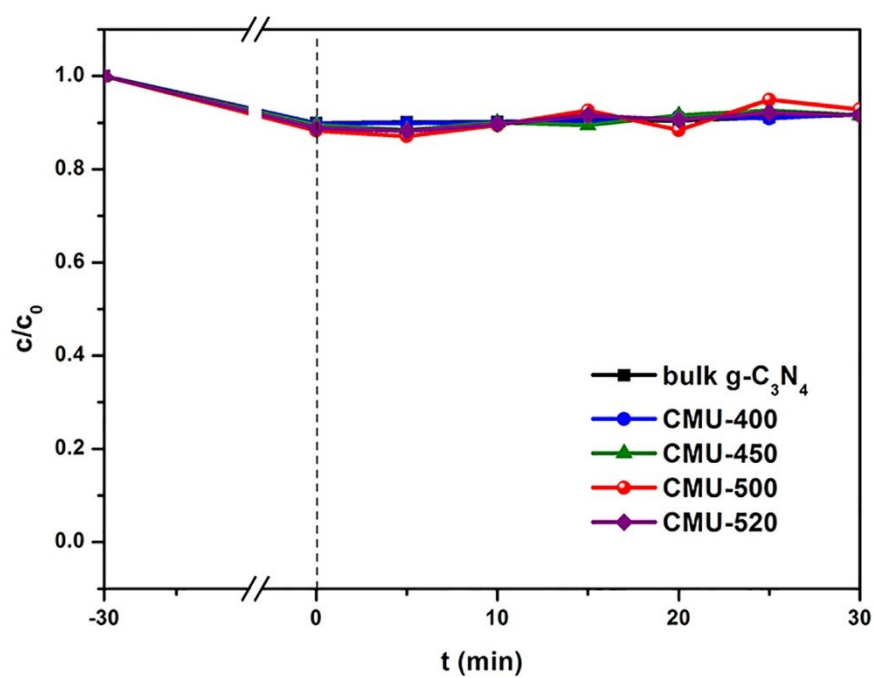


Figure S5. The concentration changes of Cr(VI) as a function of irradiation time with single different catalysts under visible light irradiation ($\lambda > 420$ nm).

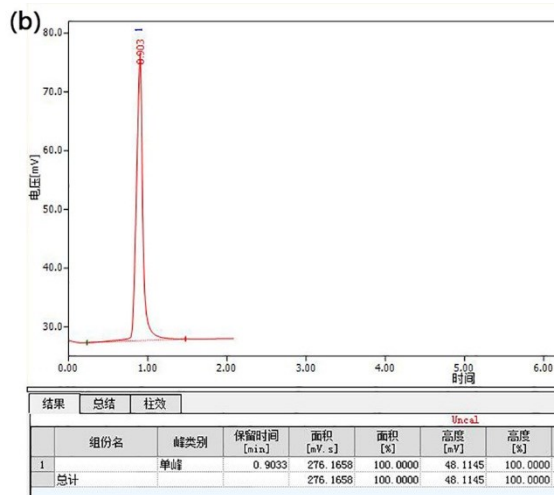
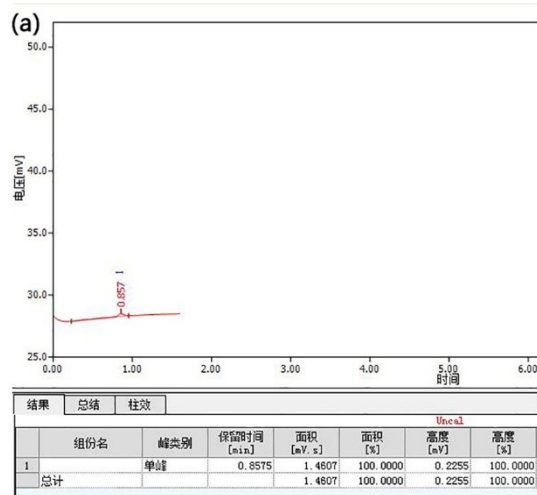


Figure S6. The Gas chromatogram of catalyst after hydrogen production for 4 h. (a) bulk g-C₃N₄ and (b) CMU-500.

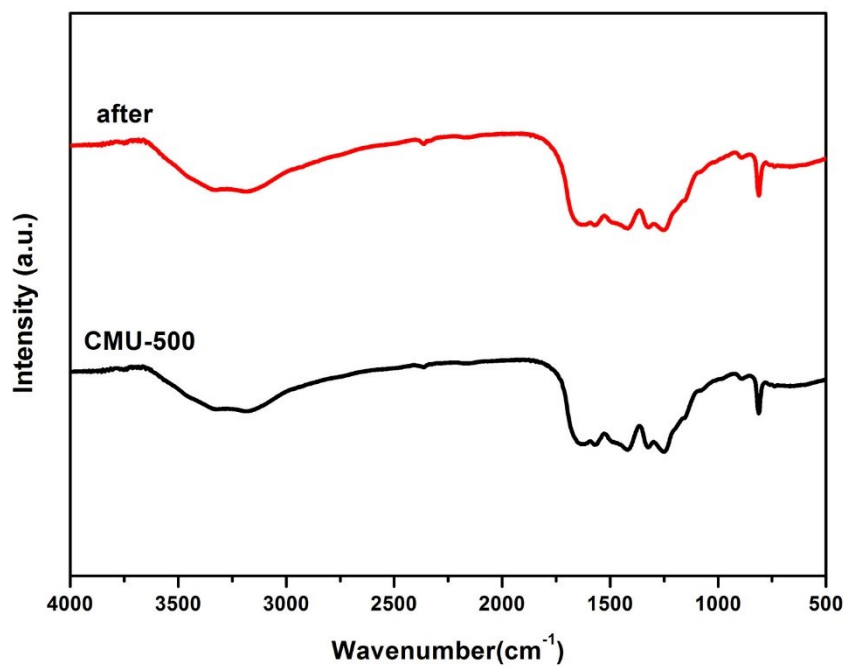


Figure S7. FT-IR analysis of CMU-500 after 4th run cycle photocatalytic experiments.

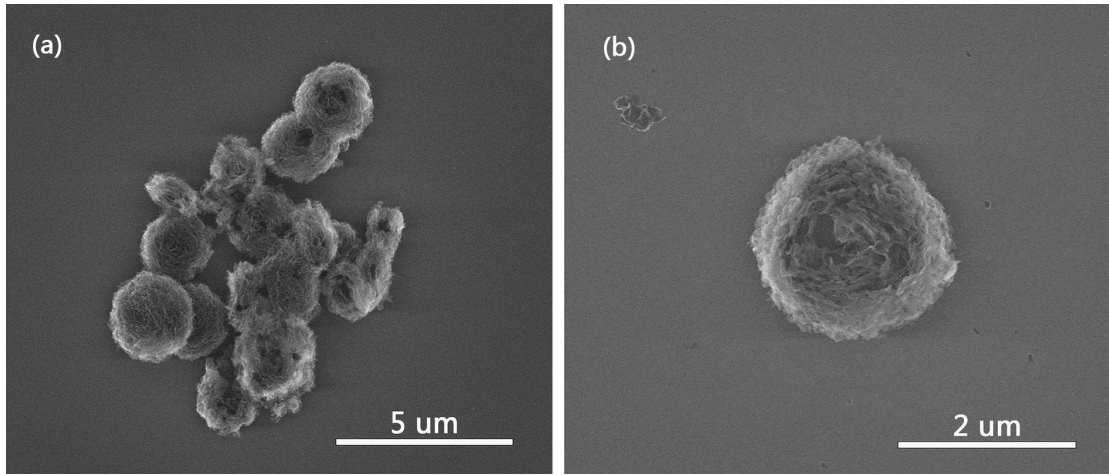


Figure S8. SEM images of CMU-500 having hollow erythrocyte-like structure after photocatalytic reaction.

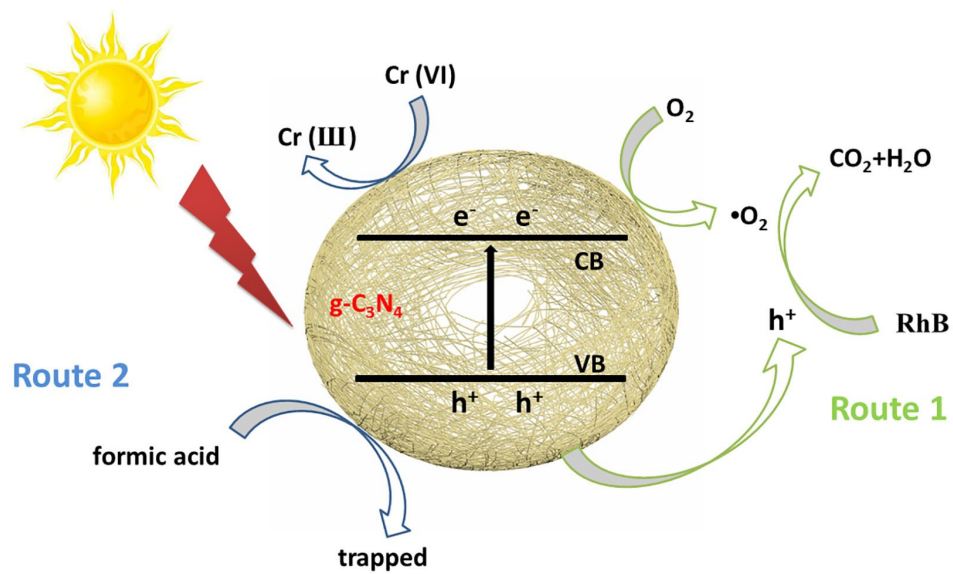


Figure S9. A possible mechanism diagram for removing pollutants.